Journal of Cleaner Production 334 (2022) 130205

Contents lists available at ScienceDirect

Journal of Cleaner Production

journal homepage: www.elsevier.com/locate/jclepro

Cleaner production of proso millet (*Panicum miliaceum* L.) in salt-stressed environment using re-watering: From leaf structural alleviations to multi-omics responses

Yuhao Yuan, Jiajia Liu, Qian Ma, Yongbin Gao, Qinghua Yang, Xiaoli Gao **, Baili Feng *

State Key Laboratory of Crop Stress Biology for Arid Areas, College of Agronomy, Northwest A & F University, Yangling, Shaanxi, China

ARTICLE INFO

Handling Editor: Prof. Jiri Jaromir Klemeš

Keywords:
Proso millet
Phenotypic
Microstructural
Plant hormones
Omics integration
Re-watering

ABSTRACT

Severe environmental conditions inhibit plant growth, which is rapidly restored when conditions improve. However, the mechanisms underlying re-watering to relieve Na^+ toxicity and promote growth in proso millet are unclear. Herein, comparative phenotypic, physiological, phytohormone and multi-omics analyses between salt-sensitive (SSR) and salt-tolerant (STIM) proso millet cultivars were performed under salt stress and subsequent re-watering. Phenotypic and physiological analyses suggested that the accumulation of biomass and growth rate of STIM were not only higher after stress recovery than SSR but also higher than its control condition (STIM_CK), showing a compensation effect. A microstructural analysis indicated that STIM maintained a better surface structure, internal structure, and chloroplasts after stress recovery compared with its reactions under salt stress. A phytohormone analysis showed that the jasmonic acid (JA) and jasmyl-L-isoleucine (JA-Ile) contents specifically and significantly increased in STIM under salt stress and recovered with re-watering. Transcriptome analysis suggested that 3160 differentially expressed genes (DEGs) (1671 DEGs were downregulated, and 1589 DEGs were upregulated) and 1319 DEGs (565 DEGs were downregulated, and 751 DEGs were upregulated) were specifically identified in STIM under salt stress and re-watering, respectively, whereas 6184 DEGs (2666 DEGs were downregulated, and 3518 DEGs were upregulated) and 2721 DEGs (1175 DEGs were downregulated, and 1546 DEGs were upregulated) were detected in SSR. Proteomes analyses showed that up to 38.28% and 44.68% of proteins were individually expressed specifically at the protein level in SSR under salt stress and subsequent re-watering, respectively, and 43.56% and 39.31% in STIM, respectively, indicating the involvement of post-transcriptional regulation under salt stress and subsequent re-watering. Subsequently, the functions of commonly regulated DEGs and differentially expressed proteins (DEPs) were analyzed, which were significantly enriched in photosynthesis and porphyrin and chlorophyll metabolism pathways. Therefore, this study provides guidelines for phytoremediation and utilization of saline soils, and cleaner crop production.

1. Introduction

Long-term climate change and periodic environmental extremes threaten the global crop yield and food security and impede the sustainable development of modern agriculture (Cappelli et al., 2015; Gupta et al., 2020). These challenges are exacerbated by soil salinization caused by natural or human activities, leading to more serious land degradation (Metternicht and Zinck, 2003; Shi et al., 2009; Zhang et al., 2021). Once salinized agricultural lands become established, is difficult to manage them, and the land is often abandoned (Cuevas et al., 2019). Thus, it is critical to practice a sustainable strategy to manage and utilize salinized soil. Salt-tolerance plant cultivation is highly appropriate for salt-affected soil usage owing to both economic benefits and soil amelioration effects (Han et al., 2015; Lu et al., 2021). However, most plants are salt-sensitive and cannot complete a life cycle under high salt concentrations (Flowers et al., 2015; Zelm et al., 2020). Proso millet (*Panicum miliaceum* L.) is widely cultivated as a traditional crop in arid and semi-arid regions around the world (Habiyaremye et al., 2017). This crop possesses unique features for resilience to adverse environments, particularly under infertile soil conditions (Dawson et al., 2019). In

* Corresponding author. State Key Laboratory of Crop Stress Biology for Arid Areas, College of Agronomy, Northwest A & F University, Yangling, Shaanxi, China.
** Corresponding author. State Key Laboratory of Crop Stress Biology for Arid Areas, College of Agronomy, Northwest A & F University, Yangling, Shaanxi, China.
E-mail addresses: gao2123@nwsuaf.edu.cn (X. Gao), fengbaili@nwsuaf.edu.cn (B. Feng).

https://doi.org/10.1016/j.jclepro.2021.130205
Received 10 July 2021; Received in revised form 19 November 2021; Accepted 18 December 2021
Available online 22 December 2021

addition, the C_4 photosynthesis, short life cycle, and salt tolerance of proso millet make it a very promising model crop to study salt stress responses (Zou et al., 2019; Yuan et al., 2021). Moreover, it is considered to have the highest water-use efficiency, thus, supporting more water-efficient agriculture (Zou et al., 2019). Therefore, it is necessary to comprehensively reveal the mechanism for the salt tolerance of proso millet to ensure the safety of energy and food crops and enable sustainable agricultural development.

As sessile organisms, plants must adjust their growth and development to withstand environmental stresses, such as salt and drought (Zhu et al., 2016; Yang and Guo, 2018). However, when conditions improve, such as following rainfall or irrigation, plants switch to a rapid compensatory growth recovery phase from the salt stress response phase (Li et al., 2020a). Therefore, plants are frequently subjected to cycles of stress and re-watering. Plants facing stress adjust their growth to withstand the adverse growth conditions (Yang and Guo, 2018). For instance, growth inhibition, which as an effective adaptive strategy to maximize survival (Zhang et al., 2020). However, plants exhibit different degrees of growth and changes (from morphological and physiological change to the regulation of gene expression) after stress relief through re-watering or dilution (Javed et al., 2018; Jia et al., 2020; Li et al., 2020b; Tan et al., 2020). Notably, resilience primarily depends on the degree and duration of the previous stress and the species (Xu et al., 2010). Furthermore, most plants can completely recover under moderate stress, while only a few can completely recover under severe stress (Xu et al., 2010; Wang et al., 2020). However, most of the research on re-watering has focused on revealing the mechanism of re-watering after drought stress (Gao et al., 2015; Jia et al., 2020; Erdal et al., 2021; Yu et al., 2021). Moreover, although re-watering can promote plant growth by relieving Na^+ toxicity, which compensates for the prior loss to a certain degree (Javed et al., 2018), only a few studies have reported on the molecular mechanism of re-watering after stress compared with the physiological response studies (Xu and Wu, 2013; Azeem et al., 2017; Li et al., 2020a). Therefore, there is an urgent need for a specific study of the molecular basis of this post-recovery growth and physiological traits. An integrated analysis of transcriptomic and proteomic changes can provide a comprehensive overview of the underlying mechanisms of resistance to salt stress and subsequent mitigation by re-watering. To our knowledge, few studies has reported research on transcriptomic and proteomic evidence, particularly that associated with proso millet grown under salt stress and subsequent re-watering.

In this study, two proso millet cultivars with contrasting salt tolerance attributes, SSR (salt-sensitive) and STIM (salt-tolerant), were selected to assess their comparative phenotypes, physiological characteristics, microstructure, and multi-omics (transcriptomic and proteomic) under salt stress and subsequent re-watering. The aims of the study were (1) to identify how re-watering regulates the growth and compensation effect of proso millet; (2) to investigate the response of microstructures to re-watering using field-emission scanning electron microscopy, paraffin sections, and transmission electron microscopy; and (3) to reveal the molecular basis of salt stress and subsequent re-watering mechanisms in proso millet by an integrated analysis of the transcriptome and proteome. Accordingly, cultivating crops in salt-stressed environment with re-watering alleviation is a good trial for cleaner crop production in terms of saving water resource, utilizing saline soils, and alleviating the potential risks. The findings of this work will provide useful information on the phytoremediation and utilization of saline soils, and cleaner crop production.

2. Materials and methods

2.1. Plant material and growth conditions

Two proso millet cultivars, SSR (salt-sensitive) and STIM (salt-tolerant), were obtained from the College of Agronomy, Northwest A&F University, Yangling, China. Experiments were conducted in an environmentally-controlled greenhouse (temperature: 28/18 °C day-night; relative humidity: 60%; and 14 h photoperiod). Uniform and healthy seeds of SSR and STIM were surface-sterilized using 0.1% $HgCl_2$ for 5 min, washed three times with sterile water, and subsequently germinated. The seedlings were transferred to a hydroponic system one week after germinating and then grown in ½ Hoagland's nutrient solution. After two weeks, the seedlings were treated with ½ Hoagland's nutrient solution containing 0 mM (control, CK) and 170 mM NaCl (ST) for a week. The roots were then rinsed in distilled water, and the seedlings were-planted in ½ Hoagland's nutrient solution for a week (re-watering, RW). Plants were harvested and analyzed at the end of the salinity (salt stress) and release phase (re-watering). The hydroponic solution was controlled by monitoring the pH and electrical conductivity (EC). The culture solutions were changed every 2 d throughout the growth period.

2.2. Plant growth

Shoot and root biomass accumulation (g fresh weight) were determined after harvesting by weighing individual plants. The mean growth rate (MGR) (g d^{-1}) was estimated using the equation: $[(FW_2–FW_1)/(t_2-t_1)]$, where FW_2 and FW_1 are fresh weights, and t_2 and t_1 are the end and the start of the time, respectively.

2.3. Water content

The roots and the third completely developed leaves of each plant were harvested from the control, salt stress-treated (7 d), and re-watering-treated plants (7 d) to determine the content of water. The tissues were then dried at 60 °C for 72 h. The water content (g DW^{-1}) was calculated as follows: [(FW-DW)/DW], where FW and DW are the fresh and dry weights, respectively.

2.4. Histochemistry and ion leakage

Fully expanded third leaves (the third knob) of each plant were harvested from the control, salt stress-treated (7 d), and re-watering-treated plants (7 d) for histochemistry. The dead cells were stained with Trypan blue staining as described by Qiao et al. (2010). Moreover, the relative electrolyte leakage (EL) was evaluated as described by Su et al. (2015) to quantify cell death.

2.5. Microscopy

Leaflets from the third fully-expanded leaf of SSR and STIM were harvested from the control, salt stress-treated (7 d), and re-watering-treated (7 d) plants for microscopy. The leaves were cut, prepared as described by Pan et al. (2012), and dried in a critical-point drying machine (Emitech K850; Quorum, UK). The surface structure was observed using an S-4800 field-emission scanning electron microscope (Hitachi, Ltd., Tokyo, Japan) after metal spraying. Paraffin sections of the leaves were prepared as described by Qi et al. (2014) to examine the leaf cell structure. Briefly, leaves were cut and subjected to the experimental process, including dehydration, dip waxing, embedding, slicing, and safranin O-fast green staining. An epifluorescence microscope (Carl Zeiss, Ober-Kochen, Germany) was used to visualize and image the changes in leaf structure. The leaves were prepared for transmission electron microscopy (TEM) as described by Meng et al. (2014).

2.6. Quantitative analysis of hormones via LC-MS/MS

2.6.1. Hormone extraction

Twenty-four plant hormones were assayed as described by Zhang et al. (2016). These included auxin (methyl 3-indolyl acetate [ME-IAA]; N6-isopentenyl adenosine [IPA]; indole-3-acetic acid [IAA];

3-Indolebutyric acid [IBA]; indole-3-carboxaldehyde [ICA]), cytokinins (N6-Isopentenyladenine [IP]; trans-Zeatin [tZ]; cis-Zeatin [cZ]; dihydrozeatin [DZ]; tZR, trans-Zeatin-riboside [tZR]), jasmonic acid (jasmonic acid [JA]; dihydrojasmonic acid [H2-JA]; methyl jasmonate [Me-JA]; jasmonoyl-L-isoleucine [JA-Ile]), salicylic acid [SA]; methyl salicylate [Me-SA]), abscisic acid (ABA), 1-aminocyclopropanecarboxylic acid (ACC), gibberellin (GA1, gibberellin A1 [GA1]; GA3, gibberellin A3 [GA3]; GA4, gibberellin A4 [GA4]; GA7, gibberellin A7 [GA7]), and brassinolide (BL). The leaf surfaces were cleaned using phosphate buffer saline (PBS, pH 7) and ground into powder by freeze-drying. A total of 25 mg of each sample was transferred to an Eppendorf tube. A volume of 1000 μL of extract solution (50% acetonitrile in water, pre-cooled at −40 °C, containing isotopically-labeled internal standard mixture) was added to the samples, vortexed for 30 s, sonicated in an ice-water bath for 5 min, and homogenized at 40 Hz for 4 min. The homogenization and sonication were repeated twice. The samples were centrifuged at 4 °C for 10 min at 12000 rpm) to obtain the supernatant. An aliquot (800 μL) of the supernatant was purified by solid-phase extraction (SPE). The SPE cartridges were washed using 1 mL of methanol and equilibrated with 1 mL 50% ACN/H_2O (v/v). The samples (supernatant obtained as described above) were loaded, and then the flow-through fraction was discarded. The cartridge was then rinsed using 1 mL of 60% ACN/H_2O (v/v). The samples were then evaporated to dryness under a gentle stream of nitrogen and reconstituted in 100 μL of 10% ACN/H_2O (v/v). All the samples were vortexed for 30 s, sonicated in an ice-water bath for 5 min and then centrifuged at 4 °C for 15 min at 12,000 rpm). The clear supernatant was then subjected to ultra-high-performance liquid chromatography-tandem mass spectrometry (UHPLC-MS/MS).

2.6.2. UHPLC-MS/MS analysis

An EXIONLC System (Sciex) with a Waters ACQUITY UPLC CSH C18 column (150 × 2.1 mm, 1.7 μm, Waters, Milford, MA, USA) was used for UHPLC analysis. The mobile phase, A, contained 0.01% formic acid in water, while the mobile phase, B, had 0.01% formic acid in acetonitrile. The column and auto-sampler temperatures were 50 °C and 4 °C, respectively, and the injection volume was 5 μL. A SCIEX 6500 QTRAP$^+$ triple quadrupole mass spectrometer (Sciex) with an IonDrive Turbo V electrospray ionization (ESI) interface was used for assay development. Typical ion source parameters were: Curtain Gas. 40 psi; Ion Spray Voltage, ±4500 V; temperature, 475 °C; Ion Source Gas 1, 30 psi; and Ion Source Gas 2, 30 psi. The MRM parameters for each of the targeted analytes were optimized using flow injection analysis. The standard solutions of the individual analytes were injected into the API source of the mass spectrometer. Several most sensitive transitions were used in the multiple reaction monitoring (MRM) scan mode to optimize the collision energy for each Q1/Q3 pair. SCIEX Analyst Work Station Software (Version 1.6.3) and Sciex MultiQuant™ 3.0.3 were used for the quantitative analysis. The concentration of plant hormones was determined as described by Simura et al. (2018) as follows:

$$CM[\mathrm{nmol}/kg] = \frac{CC[nmol/\mathrm{L}] \times \mathrm{DiL} \times V[\mu L]}{m[mg]}$$

Where *CM* represents the metabolite concentration; *CC* represents the concentration directly measured by the instrument; *DiL* represents dilution factor, while *V* represents the final volume.

2.7. Transcriptome sequencing analysis

Allwegene (https://www. allwegene.com/) was used for RNA extraction, cDNA library construction, high-throughput sequencing, raw data processing, and bioinformatics analysis. Briefly, 3 μg of RNA was used for library generation via the NEBNext® Ultra™ RNA Library Prep Kit for Illumina® (#E7530L, NEB, Ipswich, MA, USA). All 18 transcriptome libraries (control group, salt treatment group, and re-watering group) were sequenced on an Illumina HiSeq™ 4000 platform (Illumina, San Diego, CA, USA) to generate 150 bp paired-end reads. TopHat (v2.1.1) (Trapnell et al., 2012) was used to align the reads to the genome of *Panicum miliaceum* L., then assembled using Cufflinks (v2.2.1) (Trapnell et al., 2012). Differentially expressed genes (DEGs) were assessed using Cuffdiff (Trapnell et al., 2012), identified via DESeq (Anders and Huber, 2010) with the false discovery rate (FDR) < 0.05 and log2 |fold-change| > 1. The DEGs were then used for the enrichment analyses of Gene Ontology (GO) (http://bioinfo.cau.edu.cn/agriGO/) and the Kyoto Encyclopedia of Genes and Genomes (KEGG) pathway (https://www. kegg.jp/kegg/pathway.htmL). A corrected *P*-value <0.05 was set as the significance threshold (Mao et al., 2005; Young et al., 2010).

2.8. Protein extraction and digestion

2.8.1. Sample preparation for mass spectrometry

Treated leaf tissues were immediately frozen in liquid nitrogen. The proteins were extracted as described by Wang et al. (2017). The samples were ground to a powder in liquid nitrogen and dissolved in lysis solution (500 mM Tris-HCl buffer, 50 mM ethylenediaminetetraacetic acid, 700 mM sucrose, 100 mM KCl, 2% β-mercaptoethanol, 1 mM phenylmethylsulfonyl fluoride, and 1% v/v trypsin) for 10 min. A water bath-type sonicator (Bioruptor UCD-200; SONIC BIO Co., Kanagawa, Japan) was used to mix the samples in Tris-saturated phenol as follows: 10 min in 30 s on/30 s off cycles, followed by centrifugation at 4 °C for 10 min at 5500 g. The supernatant was extracted in cold acetone, precipitated at −20 °C overnight, then centrifuged at 4 °C for 10 min at 5500 g, and the supernatant was discarded. The precipitate was dissolved in 4% sodium dodecyl sulfate (SDS). A BCA Protein Assay Kit (Beijing Solarbio Science & Technology, Beijing, China) was used to measure protein concentration following the manufacturer's instructions. SDS-PAGE was then used to check for contamination and degradation in the proteins.

The proteins were digested using the FASP method (Wisniewski et al., 2009). Sample proteins (100 μg each) were diluted by adding 8 mM urea to 200 μL. Sample proteins were then added to 10 mM dithiothreitol at 56 °C for 30 min and subjected to alkylation with 30 mM iodoacetamide at room temperature in the dark for 40 min. The solution was then transferred to a 10 K ultrafiltration tube, and then centrifuged at 12,000 g at room temperature to remove the filtrate. A volume of 400 μL of 8 M urea was then added to the filter unit and centrifuged at 12000 g for 15 min. The procedure was conducted in triplicate. A volume of 200 μL of 50 mM NH_4HCO_3 was also added to the filter unit and centrifuged at 12,000 g for 10 min (three times). Finally, trypsin (Promega, Madison, WI, USA) was added at a 50:1 (protein: trypsin mass ratio) for digestion at 37 °C for 16 h. The filtrate was collected after centrifugation (12,000 g, 4 °C, for 10 min). The sediment was then freeze-dried for LC-MS/MS analysis. The cells were lysed in SDC buffer, followed by sonication, protein quantification, reduction, alkylation, and desalting using SDB-RPS StageTips (described above) to generate the spectral library for data-independent acquisition (DIA) measurements. High pH reversed-phase chromatography was used to fraction 8 μg and 30 μg of the peptides into eight and 24 fractions, respectively, as described by Kulak et al. (2017). The fractions were automatically concatenated by shifting the collection tube during the gradient, dried in a vacuum centrifuge, and resuspended in buffer A* (0.2% TFA/2% ACN).

2.8.2. LC-MS/MS measurements

The peptides were directly injected into a home-packed column (150 m × 15 cm, ReproSil-Pur C18-AQ, 1.9 μm, Dr. Maisch GmbH, Ammerbuch, Germany) with an integrated spray-tip. The proteins were then separated using a 180 min gradient of solvents A (0.1% [v/v] formic acid [FA] in water) and B (0.1% [v/v] formic acid [FA] in 80% acetonitrile [ACN]) (from 5 to 13% B in 13 min, from 13 to 30% B in 145 min, from

30 to 45% B in 15 min, from 45 to 95% B in 1 min, and held at 95% B for 6 min) at 600 nL/min. The mass spectrometer was operated at the Top10 data-dependent mode (DDA) with a full scan range of 300 to 1650 m/z at a resolution of 60,000 with automatic gain control (AGC) target of 3e6 and a maximum fill time of 20 ms. Precursor ions were isolated with a width of 1.4 m/z and fragmented via higher-energy collisional dissociation (HCD) (normalized collision energy [NCE] 27%). The fragments were scanned at a resolution of 15,000, an AGC of $1e^5$, and a maximum injection time of 60 ms. Dynamic exclusion was enabled and set to 30 s. A full MS resolution was set at 120,000 with a full scan range of 300 to 1650 m/z, a maximum fill time of 60 ms, and an AGC target of 3e6 for DIA measurements. One full scan was followed by 12 windows with a resolution of 30,000 in profile mode. A stepped HCD (NCE 25.5, 27, and 30%) was used to fragment the precursor ions.

2.8.3. Mass spectrometer data and functional enrichment analysis

The Scaffold DIA (Proteome Software, Inc., Portland, OR, USA) search engine was used for MS data analysis via the chromatogram library (Kawashima et al., 2019). A peptide or protein FDR <1% was set as the protein identification threshold. The peptides were quantified using the Encyclope DIA algorithm in Scaffold DIA. The false discovery rate (FDR) was adjusted to <0.01. The differentially expressed proteins (DEPs) were identified using mapDIA after 7 d of salt treatment and recovery by comparing the expression levels with the control (Teo et al., 2015). Genes with a minimum of 2-fold change (|log2 (FC) |≥1) and a false discovery rate (FDR) of $p \leq 0.05$ were identified as DEGs. The GOseq R package (v1.12) and KEGG Orthology Based Annotation System software (KOBAS, v2.0) were used to determine the DEPs in GO and KEGG pathways, respectively. A corrected *P*-value <0.05 was considered the significant cutoff value (Young et al., 2010).

3. Results

3.1. Re-watering relieves salt-induced growth inhibition

Salt stress significantly inhibited the growth of the two proso millet cultivars (Fig. 1a). In addition, visual symptoms of damage and mortality were evident in the SSR leaves, unlike those in STIM. The shoot and root biomass of SSR under non-stressful conditions were 0.88 and 0.07 g, respectively, and 0.89 and 0.06 g, respectively, for STIM (Fig. 1b and c). After seven days of salt treatment (ST), the growth of STIM was higher in than that of SSR (Fig. 1b and c). The shoot and root biomass of STIM were 0.64 and 0.04 g, respectively, and 0.33 and 0.03 g, respectively, for SSR. Moreover, the shoot and root plant biomass of STIM was still higher than that of SSR after 7 d of salt stress recovery (RW). Remarkably, the shoot biomass accumulation of STIM (0.90 g) was also higher than that in the control (0.84 g) (Fig. 1b). In addition, the root biomass of SSR was similar before and after re-watering (Fig. 1b). Furthermore, MGRs indicated that the cultivars had different growth behaviors under salinity (Fig. 1d and e). Although the growth of the two cultivars was inhibited under salt stress, the root and shoot MGRs of STIM were still higher than those in SSR. The MGRs of STIM significantly increased (1.97-fold in the shoots and 2.11-fold in the roots) after 7 d of salt stress recovery (Fig. 1d and e), while SSR increased by 0.07 fold in shoots, and did not change significantly before and after re-watering (Fig. 1d). Notably, the shoot MGRs of STIM were also higher than those of its control condition (STIM_CK) (Fig. 1d).

3.2. Re-watering alleviates salt-induced leaf damage

Salt stress had different effects on the leaf water content in the two

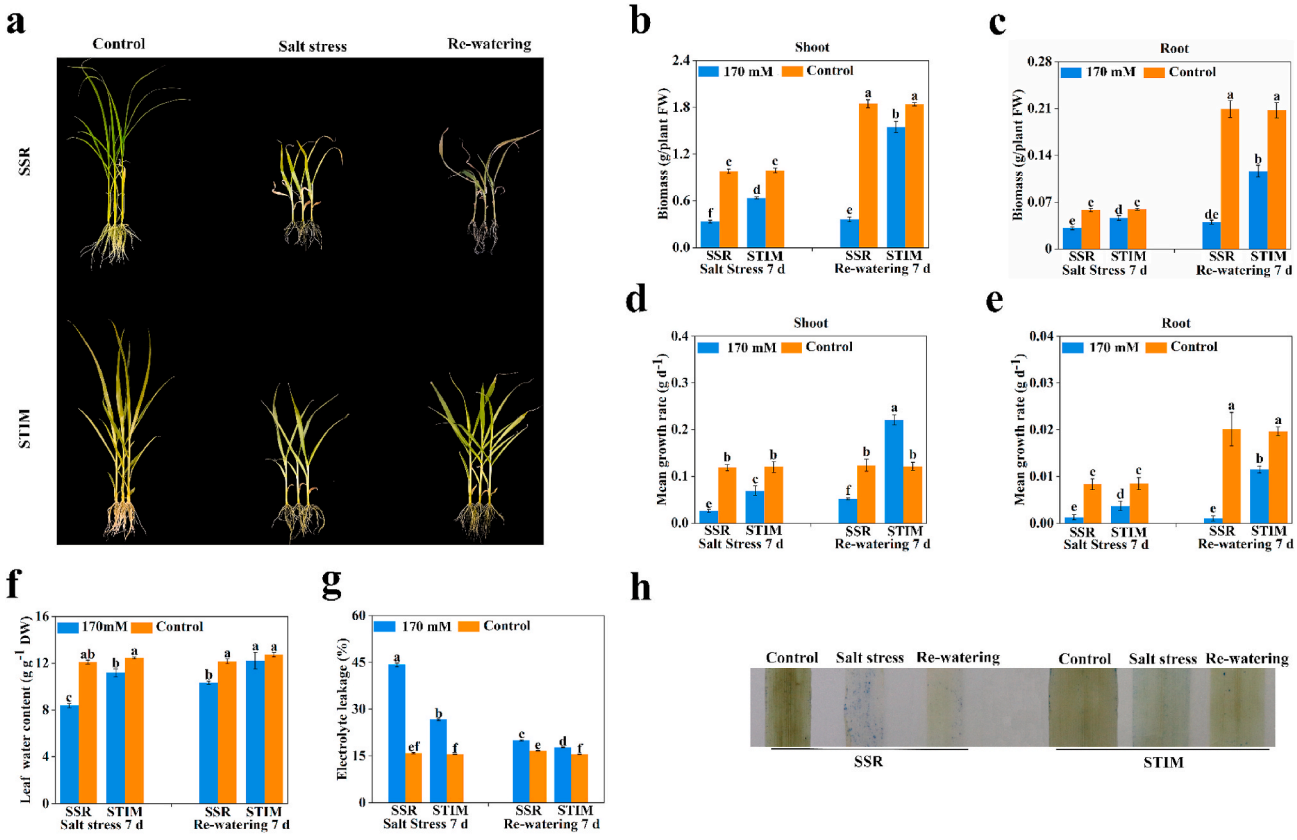

Fig. 1. Salt-induced phenotypic changes in SSR and STIM. (a) Proso millet seedlings hydroponically treated with 170 mM NaCl for 7 d, followed by recovery for 7 d. (b) Shoot biomass; (c) Root biomass; (d) Mean growth rate of the shoot (e) Mean growth rate of the root. (f) Leaf water content; (g) Electrolyte leakage. (h) Trypan blue staining of leaves. Different letters (a, b, c, d, g, h) indicate the significant differences ($P < 0.05$) between control and 170 mM NaCl. SSR, salt-sensitive cultivar; STIM, salt-tolerant cultivar.

cultivars (Fig. 1f). Although the contents of water in both SSR and STIM decreased under salt stress and progressively recovered with re-watering, STIM had higher water content. In addition, STIM recovered faster after re-watering than SSR (Fig. 1f). However, the opposite response was observed when electrolyte leakage (EL) was monitored. The relative EL analysis revealed that salt stress could damage the leaf membranes (Fig. 1g). Salt stress increased the levels of EL in SSR and STIM (2.78- and 1.72-fold, respectively). In contrast, re-watering induced low EL levels in SSR and STIM by approximately 45.20% and 66.48%, respectively (Fig. 1g). These results indicate that salt stress induces cell death in plants. The dead cells were stained with trypan blue for further visualization (Fig. 1h). The dead cells in the seedlings, leaves of the plant, and the damaged parts of the cell membrane were dark blue, indicating salt stress. In addition, the blue area of the SSR leaves was significantly larger than that of STIM under salt stress conditions (Fig. 1h). Overall, these findings suggest that the cellular activity is higher in the STIM leaves than in SSR leaves.

3.3. *Re-watering alleviates salt-induced microstructure damage in leaf*

The surface morphology, cross-cutting structure, and ultrastructure of the leaves were characterized to examine the effect of re-watering

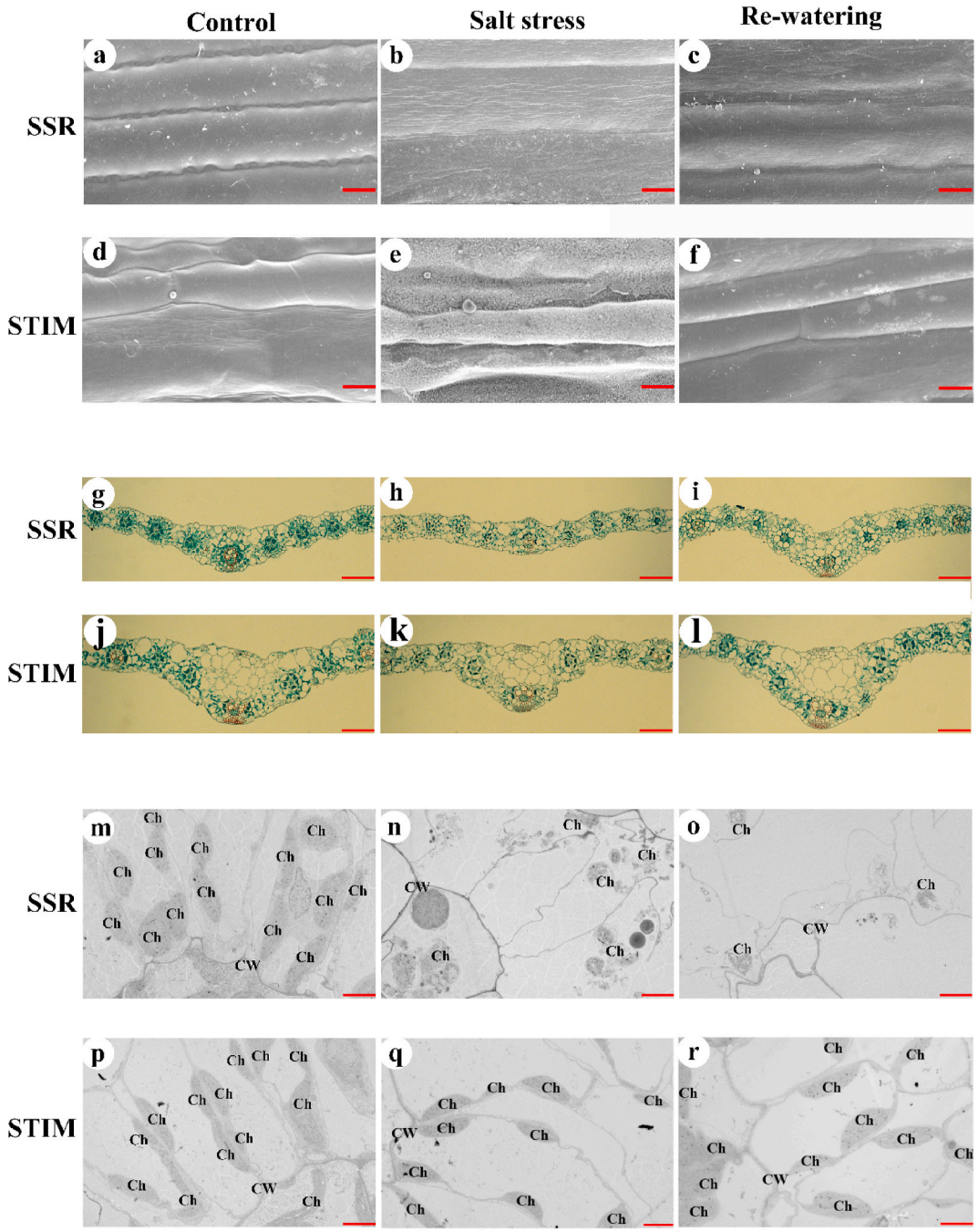

Fig. 2. Effects of re-watering and salt stress on leaf surface morphologies, paraffin sections, and subcellular structure. SEM of SSR (a, b, c); SEM of STIM (d, e, f). Root cross-section structures of SSR (g, h, i); and STIM (j, k, l). Subcellular structure of SSR (m, n, o); and STIM (p, q, r). Control, untreated leaves; salt stress-treated leaves, (170 mM NaCl treatment for 7 d); Re-watering-treated leaves (7 d). Ch, chloroplasts. CW, cell wall. a-f, 4000 magnification, scale bars = 200 μm; g-l, 100 magnification, scale bars = 200 μm; m-r, 1200 magnification, scale bars = 5 μm. SSR, salt-sensitive cultivar; STIM, salt-tolerant cultivar.

(Fig. 2). The SEM was significantly different in the leaf surface structures of the two cultivars under salt stress (Fig. 2b, e). The surface of STIM had obvious wax deposition, while that of SSR had apparent shrinkage from dehydration. However, the leaf surface of the two cultivars became smoother after re-watering (Fig. 2c, f). This an indication that re-watering maintains the integrity of the leaf surface structures by relieving Na^+ toxicity. The transverse sections of SSR and STIM leaves were also compared (Fig. 2g-l). The paraffin section images showed distorted and disordered cells with nuclear degradation in the leaves of SSR with salt stress treatments (Fig. 2h). In addition, the size of the vascular bundles of the leaves of proso millet was reduced, and the mesophyll cells of Kranz anatomy in SSR were disorderly arranged. However, re-watering alleviated cell disintegration and protoplast ruptures (Fig. 2i). Furthermore, the TEM images (Fig. 2m–r) showed that the number of chloroplasts decreased and disintegrated in SSR with the salt stress treatments, while re-watering alleviated the disintegration of chloroplasts. However, STIM only showed a decrease in the number of chloroplasts and they recovered with re-watering (Fig. 2q–r).

3.4. *Re-watering alleviates Na^+ toxicity by regulating the synthesis of plant hormone*

The LC-MS/MS absolute quantification analysis was performed on 23 plant hormones using the isotope-labeled internal standard method. The 13 plant hormones detected are shown in Table S1. The contents of ABA, IBA, ICA, GA4 and cZ significantly increased, while those of ACC, SA, and GA1 significantly decreased in both cultivars under salt stress (Fig. 3; Table S1). Alternatively, the contents of JA-Ile showed opposite changes between the two cultivars. Notably, the contents of JA and JA-Ile of STIM were specific and significantly increased in STIM under salt stress. In addition, the contents of ABA, ACC, JA, JA_Ile, IBA, ICA, GA4, and cZ decreased and recovered after re-watering in both cultivars compared with those control conditions, while the content of IPA increased and recovered. In particular, most of the hormone contents returned to a level similar to the control in STIM, including ABA, H2_JA, JA_Ile, IAA, IBA, ICA, and IPA In contrast, the contents of four of them (ABA, H2_JA, ICA, and IPA) were still significantly higher in SSR than in the control. These results indicated that STIM initiated more hormones in response to salt stress than SSR did and effectively recovered with re-watering.

3.5. *Re-watering triggers transcriptome reprogramming*

The effect of re-watering on transcriptomes was assessed by comparing the transcriptomes of both proso millet leaves (salt stress/re-watering) to comprehensively reveal the mechanism underlying the detoxification of Na^+ toxicity. Pearson correlation coefficient (PCC) and principal component analysis (PCA) were conducted based on the average fragments per kilobase of transcript per million mapped fragments (FPKM) values for all the expressed genes in at least one of the eight samples to assess the transcriptional response of SSR and STIM to salt stress and re-watering (Fig. S1). The samples that correlated more highly in these analyses had more similar transcriptomes. As expected, the transcriptomes of the two cultivars were different under stress compared with those in the control conditions. However, all of them were similar after re-watering, indicating that re-watering promotes recovery after salt stress (Figs. S1a–b). Moreover, the genes affected in the SSR and STIM sets differed significantly after re-watering (0.91 and 0.94 correlation values for the log2 transformed data) compared with those in the control group (SSR_CK and STIM_CK). These results indicate that the transcriptomes in both proso millet cultivars have different responses to re-watering (Fig. S1a). Surprisingly, the overlap between the significantly affected transcripts (SSR_ST versus SSR_CK, STIM_ST versus STIM_CK) and re-watering (SSR_ST versus SSR_RW, STIM_ST versus STIM_RW) was low (8.20%), with only 2538 shared transcripts (Fig. 4a). In contrast, 6184 DEGs (3518 DEGs were upregulated, and 2666 DEGs were downregulated) were specifically expressed in SSR_ST versus SSR_CK, and 3160 DEGs (1589 DEGs were upregulated, and 1671 DEGs were downregulated) in STIM_ST versus STIM_CK, respectively. Alternatively, only 2721 DEG (1546 DEGs were upregulated, and 1175 DEGs were downregulated), and 1319 DEGs (751 DEGs were upregulated, and 565 DEGs were downregulated) were specifically detected in SSR_RW and STIM_RW against control conditions (Fig. 4a; Data S1). Furthermore, the genes affected in SSR and STIM differed significantly after re-watering (0.84 and 0.60 correlation values for the log2 transformed data, respectively) compared with those in the control group

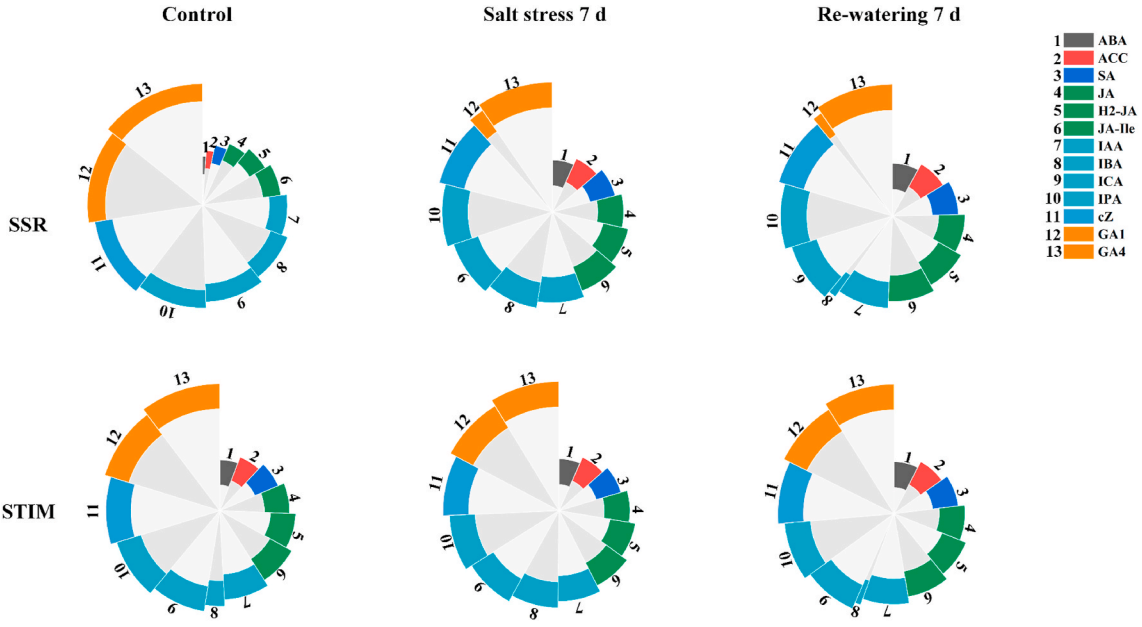

Fig. 3. Effects of re-watering and salt stress on hormone concentrations in proso millet. ABA, abscisic acid; ACC, 1-Aminocyclopropanecarboxylic acid; SA, salicylic acid; JA, jasmonic acid; H2-JA, dihydro jasmonic acid; JA-Ile, jasmonoyl-L-isoleucine; IAA, indole-3-acetic acid; IBA, 3-Indolebutyric acid; ICA, indole-3-carboxaldehyde; IPA, N6-isopentenyl adenosine; cZ, cis-Zeatin; GA1, gibberellin A1; and GA4, gibberellin A4. SSR, salt-sensitive cultivar; STIM, salt-tolerant cultivar. SSR, salt-sensitive cultivar; STIM, salt-tolerant cultivar.

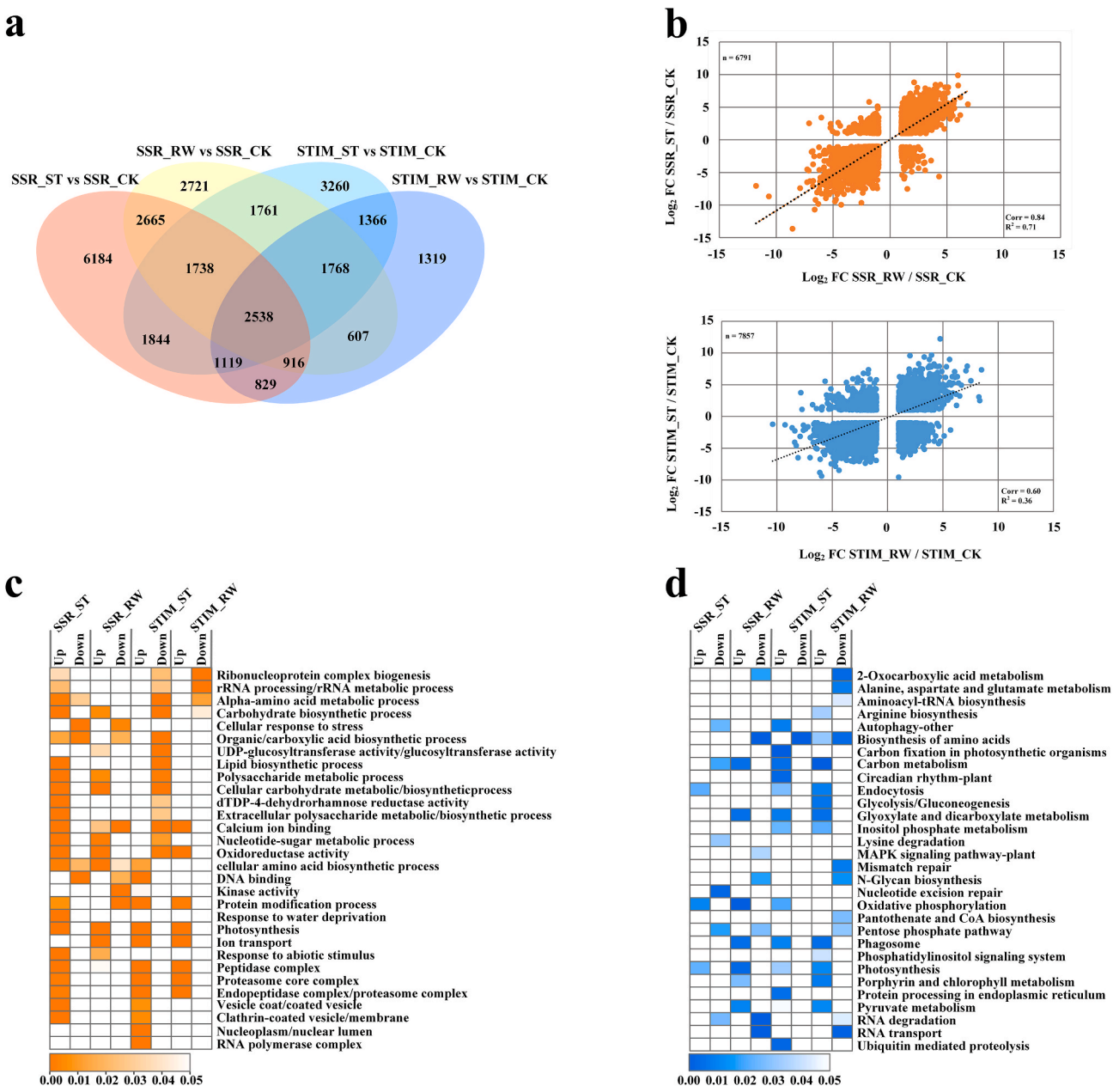

Fig. 4. Salt stress and re-watering alter the transcriptome in both cultivars of proso millets. (a) A Venn diagram shows the overlap in the numbers of transcripts consistently up or downregulated in both proso millets versus plants treated with salt stress and re-watering. (b) A scatter plot of transcripts from leaves comparing the log2 FCs in the transcript levels of the two proso millets versus those treated with salt stress and re-watering. (c) Enriched GO terms (biological processes, molecular functions, and cellular components) in down- and upregulated genes in SSR and STIM. The color scale at the bottom represents significance (corrected P-value). (d) KEGG pathways in down- and upregulated genes in SSR and STIM. The color scale at the bottom represents significance (corrected *P*-value). FC, fold-change; GO, gene ontology; KEGG, Kyoto Encyclopedia of Genes and Genomes; SSR, salt-sensitive cultivar; STIM, salt-tolerant cultivar.

(SSR_CK and STIM_CK). The results imply that the transcriptomes in both proso millet cultivars have different responses to re-watering (Fig. 4b).

GO enrichment of the significantly impacted mRNA categories is shown in Fig. 4c. There was significant over-representation of photosynthesis, peptidase complex, proteasome core complex, protein modification process, endopeptidase complex/proteasome complex, clathrin-coated vesicle/membrane, vesicle coat/coated vesicle, and cellular amino acid biosynthetic process in the SSR and STIM cultivars after treatment with salt stress. The photosynthesis and peptidase complex is continuously upregulated in plants with inhibited photosynthesis under salt stress and then activated with re-watering. Herein, the expression profiles of the DEGs in the cultivars were mapped onto the available metabolic pathways using KEGG to investigate the metabolic pathways underlying the re-watering of SSR and STIM (Fig. 4d). The hypergeometric tests revealed that several KEGG pathways were significantly altered. The upregulated genes were primarily enriched in oxidative phosphorylation, endocytosis photosynthesis, and arginine biosynthesis in both cultivars. The upregulated genes in salt stress-treated STIM were enriched in carbon fixation, circadian rhythm-plant, ubiquitin-mediated proteolysis, carbon metabolism, protein processing in the endoplasmic reticulum, glyoxylate and dicarboxylate metabolism, autophagy, phagosome, inositol phosphate metabolism, and pyruvate metabolism (Fig. 4d).

3.6. Re-watering alters the proso millet proteome

A quantitative MS strategy was used to monitor the abundances of proteins in bulk to determine the effect of re-watering on the proso millet proteome. PCC and PCA of the transcriptomes showed that salt stress and re-watering had significant effects, impacting SSR more than STIM, similar to the RNA-Seq data (Figs. S1c–d). Only 26% and 17% of the 2734 proteins measured by DIA, using the precursor ion intensities of the MS2 scans for quantification, were significantly affected in SSR and STIM, respectively, while 19% and 7.8%, respectively, were significantly affected after re-watering (Data S2) ($P \leq 0.05$ and fold-change >1.2). In addition, the overlap between the significantly affected proteins (SSR_ST versus SSR_CK, STIM_ST versus STIM_CK) and re-watering (SSR_ST versus SSR_RW, STIM_ST versus STIM_RW) was low (0.64%), with only nine shared proteins (Fig. 5a). Thus, the results indicate that salt stress and re-watering significantly affect the protein profiles more than the genotype. Furthermore, the affected proteins in SSR and STIM differed significantly after re-watering (0.72 and 0.56 correlation values for the log2 transformed data) compared with the control conditions (SSR_CK, STIM_CK) (Fig. 5b). The results imply that the proteomes of both cultivars had a similar response to salt stress and subsequent re-watering but at different degrees.

The proteome analytical results using GO are shown in Fig. 5c. The L-phenylalanine catabolic process, L-phenylalanine metabolic process, and phenylalanine ammonia-lyase activity were enriched in the SSR and STIM after salt stress treatments. The specific term enrichment for

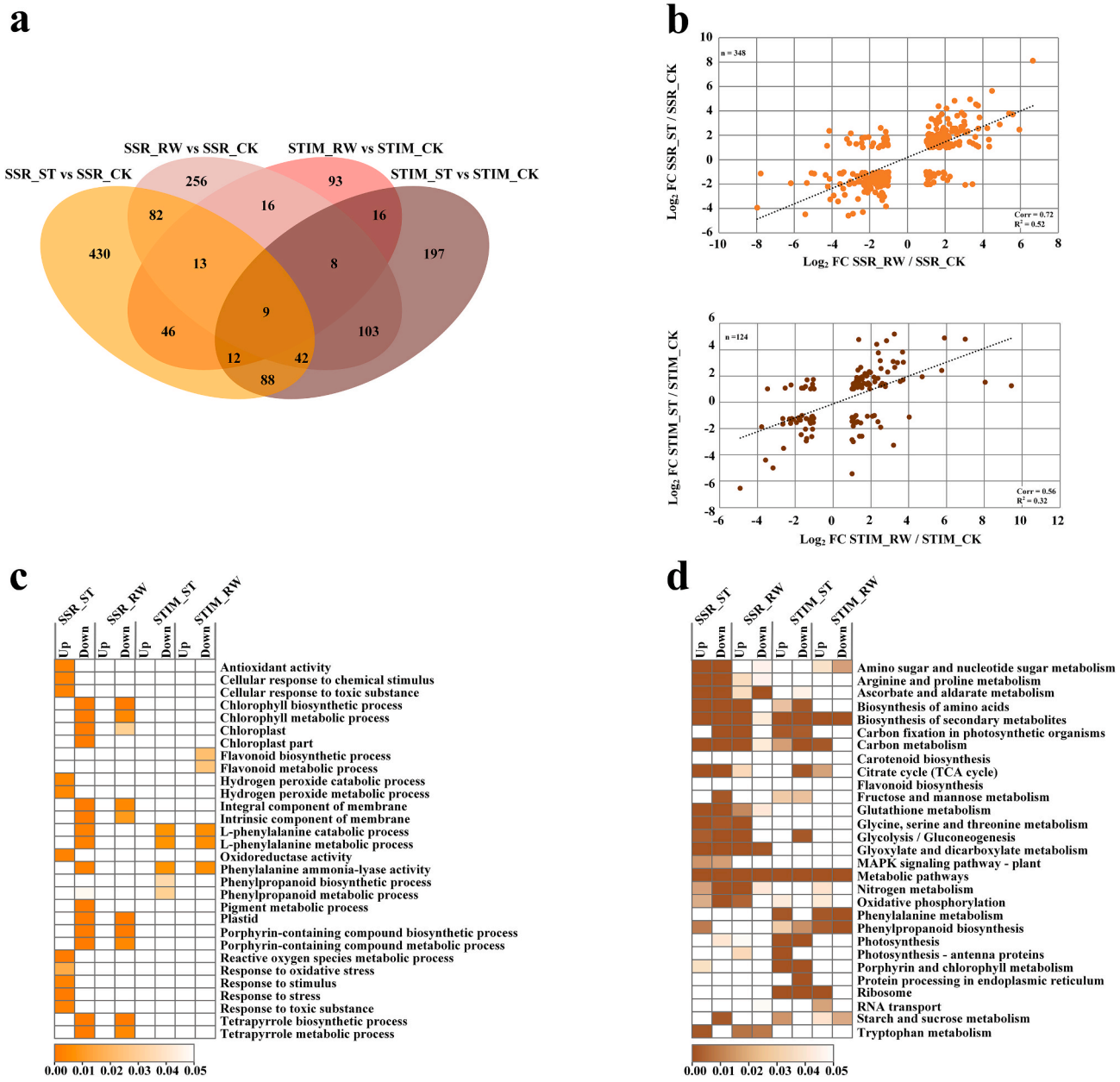

Fig. 5. Salt stress and re-watering alter the proteome in both cultivars of proso millets. (a) A venn diagram shows the overlap in the numbers of transcripts consistently up or down-regulated in both proso millets versus plants treated with salt and re-watering. (b) Scatter plot of proteins from the leaves that compare the log2 FCs in protein levels of the two proso millets versus plants treated with salt and re-watering. (c) Enriched GO terms (biological processes, molecular functions, and cellular components) in down- and upregulated proteins in SSR and STIM. The color scale at the bottom represents significance (corrected *P*-value). (d) KEGG pathways in down- and upregulated genes in SSR and STIM. The color scale at the bottom represents significance (corrected *P*-value). FC, fold-change; GO, gene ontology; KEGG, Kyoto Encyclopedia of Genes and Genomes; SSR, salt-sensitive cultivar; STIM, salt-tolerant cultivar.

SSR_ST versus SSR_CK included the response to oxidative stress, stimulus, stress, and toxic substances. Notably, no term was enriched in SSR_RW versus SSR_CK and STIM_RW versus SSR_CK, indicating that re-watering substantially promotes restoration after salt stress. The KEGG pathways represented by all the assembled proteins were predicted to further determine the role of metabolic pathways in the re-watering process. The top 30 KEGG pathway enrichments are shown in Fig. 5d. The pathways enriched between SSR_ST versus SSR_CK and STIM_ST versus STIM_CK were only those in the biosynthesis of amino acids and secondary metabolites, indicating that the two cultivars have different pathways for salt stress response. However, phenylalanine metabolism and phenylpropanoid biosynthesis were significantly enriched in STIM after re-watering (Fig. 5d), indicating that STIM inhibits Na^+ toxicity via the modulation of cell wall biosynthesis.

3.7. Proteome/transcriptome comparisons identify processes affected by re-watering

The full transcriptome and proteome data sets were compared (salt stress versus re-watering) to assess the effect of re-watering on Na^+ toxicity (Fig. 6). The log2 fold changes between salt stress and the control of the two cultivars, and their between re-watering and control conditions in the transcriptome and proteome data sets were compared (Fig. 6a–d). A scatter plot of these relationships was then subdivided into sectors, and each was assessed for gene ontology terms that showed a significant change in gene levels only (blue and orange), in proteins only (dark green and magenta), and in both proteins and mRNA (positively correlated, green and red; negatively correlated, dark yellow and purple) (Fig. 6a–d). Remarkably, up to 38.28% and 44.68% of the DEPs showed significant fold-changes in SSR under salt stress and subsequent re-watering, respectively, and 43.56% and 39.31% in STIM, respectively. However, only 23.06% and 17.69% of the DEGs and DEPs simultaneously changed significantly in SSR under salt stress and subsequent re-watering, respectively, and 12.60% and 8.57% in STIM, respectively (Fig. 6a–d). These results indicate there are post-translational level changes because the change in most proteins was independent.

A total of 225 upregulated and 310 downregulated genes were altered at the mRNA and protein levels in SSR under salt stress (Fig. 6a; Data S3). The upregulated genes were enriched in nucleobase-containing small molecule metabolic process (GO: 0055086), organic acid biosynthetic process (GO: 0016053), and carboxylic acid biosynthetic process (GO: 0046394). The down-regulated genes were enriched in the organic acid biosynthetic process (GO: 0016053), organophosphate metabolic process (GO: 0055086), and small-molecule biosynthetic process (GO: 0044283) (Fig. 6e). All of these genes were enriched in nucleotide excision repair (ko03420), oxidative phosphorylation (ko00190), photosynthesis (ko00196), porphyrin, and chlorophyll metabolism (ko00860), and protein processing in the endoplasmic reticulum (ko04141) (Fig. 6i). In addition, 129 upregulated and 146 down-regulated genes were altered in STIM (Fig. 6b; Data S3). The upregulated genes were enriched in the cellular carbohydrate metabolic process (GO: 0044262), macromolecule modification (GO: 0043412), and lipid metabolic process (GO: 0006629). In contrast, the down-regulated genes were enriched in the cellular protein modification process (GO: 0006464), protein modification process (GO: 0036211), and macromolecule modification (GO: 0043412). All of these genes were enriched in the biosynthesis of amino acids (ko01230), carbon fixation in photosynthetic organisms (ko00710), protein processing in the endoplasmic reticulum (ko04141), porphyrin, and chlorophyll metabolism (ko00860). Notably, some similar functional enrichments were observed in both cultivars, including photosynthesis (ko00196), protein processing in endoplasmic reticulum (ko04141), and porphyrin and chlorophyll metabolism (ko00860). These results indicate that the pathways related to chloroplast and endoplasmic reticulum of these two cultivars are significantly affected under salt stress.

Similarly, 160 upregulated and 224 down-regulated genes changed in SSR at the mRNA and protein levels after re-watering (Fig. 6c; Data S3). The upregulated genes were enriched in transport (GO: 0006810), organophosphate metabolic process (GO: 0019637), and macromolecule modification (GO: 0043412), and the down-regulated genes were enriched in photosynthesis, light-harvesting (GO: 0009765), photosynthesis, light reaction (GO: 0019684), and photosynthesis (GO: 0015979). In addition, all of these genes were enriched in RNA transport (ko03013), Oxidative phosphorylation (ko00190), photosynthesis (ko00196), and protein processing in the endoplasmic reticulum (ko04141). Also, 61 upregulated and 113 down-regulated genes were altered in STIM after re-watering (Fig. 6d; Data S3), indicating that re-watering had restored DEGs and DEPs. In addition, the upregulated genes were enriched in mitochondrial part (GO: 0044429), translation elongation factor activity (GO: 0003746), and peptidase activity (GO: 0070011), while the downregulated genes were enriched in photosynthesis (GO: 0015979), nucleobase-containing small molecule metabolic process (GO: 0055086), and small molecule biosynthetic process (GO: 0044283). All the genes were enriched in carbon metabolism (ko01200), RNA transport (ko03013), porphyrin and chlorophyll metabolism (ko00860), and photosynthesis (ko00196). Notably, similar functional enrichments were observed in both cultivars, such as photosynthesis, protein processing in the endoplasmic reticulum, and biosynthesis of amino acids, indicating that both cultivars were severely affected under salt stress.

Furthermore, this study focused on the genes/proteins that only changed at the transcriptomic and proteomic levels in specific pathways to determine how rehydration relieves salt stress. These included pathways related to porphyrin and chlorophyll metabolism, photosynthesis, carbon fixation in photosynthetic organisms, and protein processing in the endoplasmic reticulum. Porphyrin and chlorophyll metabolism were significantly affected (Fig. 7). The porphobilinogen synthase and magnesium-protoporphyrin IX monomethyl ester cyclase were also significantly downregulated in both cultivars compared with the controls. Notably, the pheophorbide an oxygenase was overexpressed, particularly in SSR. Moreover, the chlorophyll *a* synthase was disproportionately inhibited. Collectively, these findings suggest that salt stress inhibits the synthesis of chlorophyll *a* and *b* while promoting its decomposition, thereby significantly inhibiting photosynthesis. The genes that encode proteins related to the light-harvesting complex and subunits of PSII (10 kDa polypeptide) were also substantially downregulated (Fig. 7). Similarly, various genes that encode proteins related to the photosystem and electron transport system, plastocyanin (PC), ferredoxin (Fd), and ferredoxin-$NADP^+$ reductase (FNR), were substantially downregulated. The genes that encode enzymes (carbonic anhydrase [CA], phosphoenolpyruvate carboxylase [PEPC], pyruvate/orthophosphate dikinase [PPDK], aspartate aminotransferase [AspAT]) related to C fixation were also induced. Salt stress can also cause protein misfolding or the accumulation of unfolded proteins (Fig. 7). Salt stress downregulated the gene (*CNX*) that encodes chaperones and other proteins important for enhancing the ability of proteins to fold. Salt stress also inhibited ER-associated degradation (ERAD) and protein translation suppression and enhanced the number of synthesized proteins loaded to ER via the PKR-like ER eIF2 kinase. The gene *CNX* was significantly upregulated after re-watering (Fig. 7). However, the protein disulfide-isomerase (PDIs) and eukaryotic translation initiation factor 2 subunit alpha (eIF2) were significantly inhibited.

4. Discussion

4.1. Re-watering relieves salt-induced leaf chlorosis and growth inhibition

Re-watering can recover growth characteristics in salt-stressed plants (Javed et al., 2018). This study indicated that re-watering relieved the symptoms of Na^+ toxicity and promoted growth in both cultivars. However, since plant resilience depends not only on the degree and

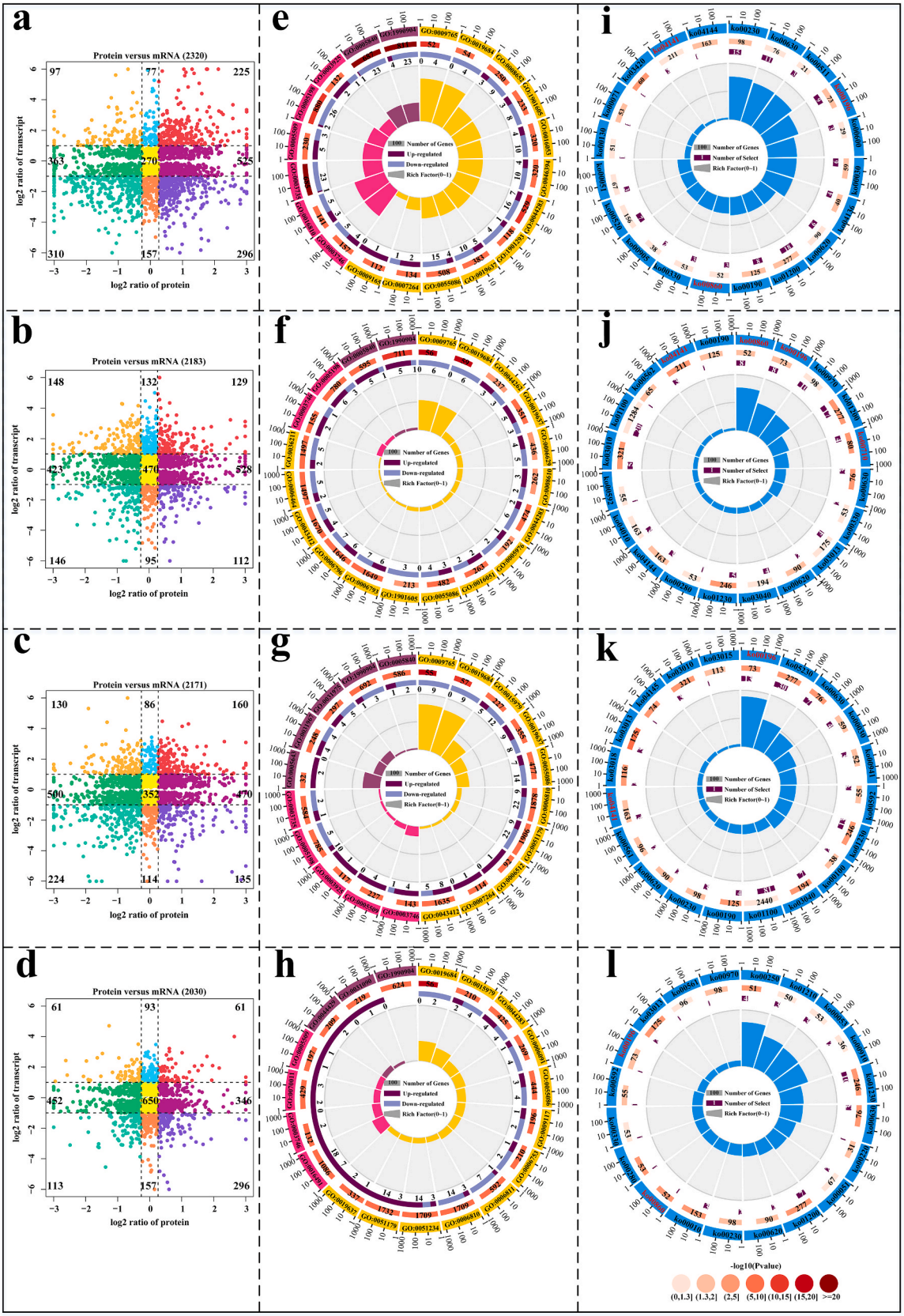

(caption on next page)

Fig. 6. Changes in mRNA and protein abundance in proso millet after re-watering. (a) A scatterplot showing the relationship between the changes in protein and mRNA abundances for 2320 proteins in SSR_ST versus SSR_CK. (b) A scatterplot showing the relationship between changes in protein and mRNA abundances for 2183 proteins in STIM_ST versus STIM_CK. (c) A scatterplot that shows the relationship between changes in protein and mRNA abundances for 2171 proteins in SSR_RW versus SSR_CK. (d) A scatterplot that shows the relationship between changes in protein and mRNA abundances for 2030 proteins in STIM_RW versus STIM_CK. A scatterplot that shows the relationship between changes in protein and mRNA abundances was drawn by plotting the log2 FC (mRNA abundance) versus the log2 FC (protein abundance). The colored sectors indicate regions that contain proteins and mRNAs whose abundances were altered two-fold: dark yellow and purple indicate that proteins and their corresponding mRNA negatively correlated; green and red indicate that proteins and their corresponding mRNA positively correlated; blue and orange show that mRNAs (but not corresponding proteins) that are more abundant; dark green and magenta indicate proteins (but not corresponding mRNAs) that are more abundant; yellow shows the co-expression of mRNAs and proteins that are not differentially expressed. (e) GO term in SSR_ST versus SSR_CK. (f) GO term in STIM_ST versus STIM_CK. (g) GO term in SSR_RW versus SSR_CK. (h) GO term in STIM_RW versus STIM_CK. (i) KEGG pathways in SSR_ST versus SSR_CK. (j) KEGG pathways in STIM_ST versus STIM_CK. (k) KEGG in SSR_RW versus SSR_CK. (l) KEGG pathways in STIM_RW versus STIM_CK. The first lap indicates the top 20 GO terms and the number of genes corresponding to the outer lap. The second lap indicates the number of the genes in the genome background and *P*-values for the enrichment of the upregulated and downregulated genes for the specified biological process. The third lap indicates the ratio of the upregulated genes (deep purple) to downregulated genes (light purple). The fourth lap indicates the enrichment factor of each GO term or KEGG pathway. GO, gene ontology. KEGG, Kyoto encyclopedia of genes and genomes. FC, fold-change; SSR, salt-sensitive cultivar; STIM, salt-tolerant cultivar.

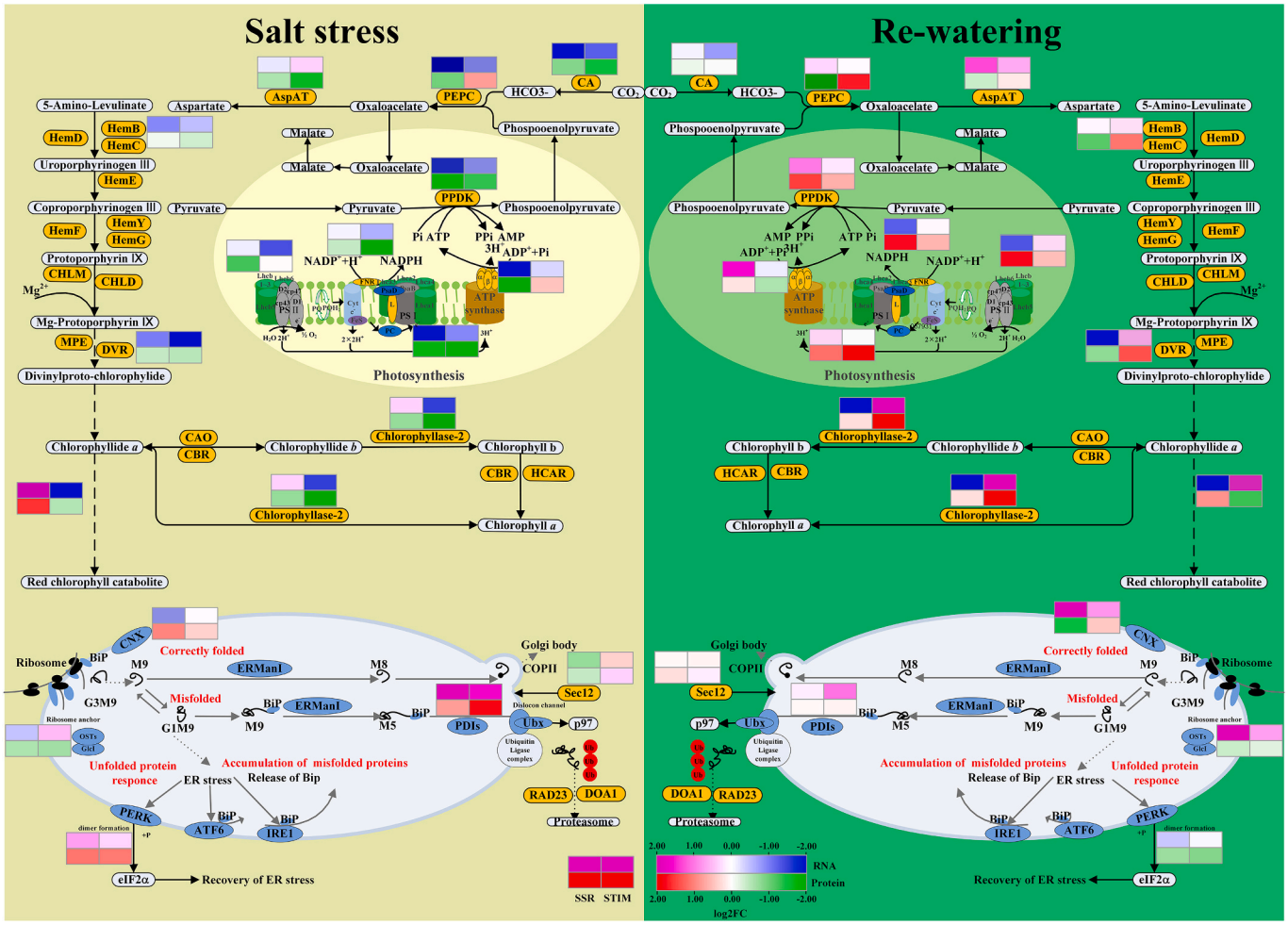

Fig. 7. Changes in porphyrin and chlorophyll metabolism, photosynthesis, and protein processing in endoplasmic reticulum after re-watering. The color block represents the value of log_2FC (ST/CK or RW/CK). Pink and red indicate upregulated genes and proteins, respectively. Blue and green indicate upregulated genes and proteins, respectively. CA, carbonic anhydrase; PEPC, phosphoenolpyruvate carboxylase; PPDK, pyruvate/orthophosphate dikinase; AspAT, aspartate aminotransferase; CNX, calnexin; Sec12, SEC12-like protein 1. DVR, divinyl reductase; PDIs, protein disulfide isomerase-like 1–5; HemB, delta-aminolevulinic acid dehydratase.

duration of previous stress but also on the cultivars (Xu et al., 2010). Thus, both cultivars exhibited different degrees of growth after stress relief through re-watering. Moreover, only a few cultivars can completely recover under severe stress (Xu et al., 2010; Wang et al., 2020). In this study, the salt-sensitive proso millet cultivar (SSR) was only increased by 0.07-fold in the shoots and did not significantly change in the root before and after re-watering. In contrast, salt-tolerant proso millet cultivar (STIM) showed compensatory growth (Fig. 1d and e). Previous studies have also reported a similar compensation mechanism for re-watering after drought (Vander et al., 2016; Niu et al., 2018). Moreover, in this study, re-watering also promoted the restoration of the regular cell membrane, reduced the leakage of electrolytes and the blue spots on the leaves similar to the findings of previous studies (Su et al., 2015). Furthermore, the leaf surface became smooth after re-watering. Re-watering also increased the numbers of parenchyma cells and chloroplasts (Fig. 2), which may be owing to the relief of Na^+ toxicity relief.

4.2. Re-watering relieves salt damage by regulating plant hormones

Numerous studies have shown that plant hormones play several biological roles in plants at different stages, in different tissues, or under different environmental conditions (Yu et al., 2020). In this study, the content of multiple hormones differed significantly after re-watering after salt stress (Fig. 3). For instance, endogenous ABA levels rapidly increased (Fig. 3) and activated sucrose non-fermenting 1-related protein kinases (SnRK2s). In contrast, the levels of endogenous SA and cZ decreased in both cultivars (Fig. 3). Similar to previous studies, the overexpression of AtNPR1 in rice was shown to accumulate very high levels of endogenous SA, enhancing sensitivity to salt and drought stresses (Silva et al., 2018). In addition, the levels of GA1 were significantly decreased compared with those of the control (Fig. 3). Notably, the changes in the hormone content in the two cultivars differed (Fig. 3). Salt stress significantly increased the contents of IAA, ICA, IPA levels in SSR, while it did not affect those in STIM (Fig. 3). Moreover, salt stress downregulated the expression of the auxin receptor-encoding genes *TIR1* and *AFB2* in STIM. Similarly, this decrease has been observed in *Arabidopsis thaliana* (Iglesias et al., 2014), indicating that both reduced auxin accumulation and downregulated expression of auxin receptors regulate the adaptation of plant growth.

4.3. Re-watering relieves Na^+ toxicity by inhibiting the degradation of chlorophyll and promoting photosynthesis

Typically, symptoms of the effect of K^+ and Na^+ imbalance are first visible in plant leaves. Herein, the effects of salt stress, including yellowing in leaves and curling in young leaflets, occurred (Albaladejo et al., 2017). Leaf chlorosis can promote the degradation of chlorophyll via salt stress (Santos, 2004). In this study, salt stress accelerated leaf yellowing (Fig. 1a). Moreover, the pheophorbide an oxygenase was overexpressed, particularly in SSR (Fig. 7). The leaf surface structure, internal structure, and chloroplast structure in STIM gradually attained normal morphology after re-watering (Fig. 2). These findings suggest that maintaining chloroplast structural integrity is essential for photosynthesis since they convert light energy into chemical energy (Staehelin, 2003). The chlorophyll (Chl) content also affects the assembly of photosynthetic reactions and chloroplast development (Hoober et al., 2007). In this study, re-watering reactivated the substantially downregulated genes that encoded proteins related to the light-harvesting complex and subunits of PSII. Various genes that encode proteins related to the photosystem and electron transport system, PC, Fd, and FNR, were also downregulated after re-watering (Fig. 7). In addition, the genes that encode proteins related to carbon fixation were reactivated, promoting the accumulation of biomass (Fig. 7), indicating that re-watering relieves salt damage by restoring higher photosynthesis and carbon fixation capabilities.

4.4. ER homeostasis plays vital roles in relieving Na^+ toxicity via re-watering

In addition to being the main site for biosynthesis and processing all of the secretory and membrane proteins in eukaryotic cells, the ER is also essential for plant adaptation to diverse environmental stresses (Liu and Howell, 2016). High salinity can easily affect the process of protein folding, triggering ER stress responses (Liu et al., 2007). In this study, molecular chaperones (SEC12-like protein 1, SEC12) were upregulated, enhancing vesicle trafficking in STIM after salt stress, thus, alleviating salt-induced ER stress processes by enhancing nascent protein folding (Fig. 7). Moreover, ER-associated degradation (ERAD) and protein translation activation accelerated the degradation of unfolded proteins (Hetz, 2012). In this study, *CNX* was significantly upregulated after re-watering, promoting the correct folding of nascent N-glycosylated proteins and endoplasmic reticulum quality control (Sarwat and Naqvi, 2013). Furthermore, eIF2α upregulates protein synthesis after ER stress via the PERK, restoring endoplasmic reticulum stress by regulating amino acid metabolism, redox, and detoxification processes (Merlot et al., 2016). Herein, it was downregulated after re-watering, indicating that re-watering relieves Na^+ toxicity by inhibiting protein misfolding, thus promoting correct folding.

5. Conclusion

This study provides comprehensive transcriptomic and proteomic analyses of the response of proso millet to re-watering. In addition to providing new insights into the post-transcriptional regulation of re-watering, this study also highlights that the system-wide rearrangement of gene and protein expression after stress recovery can enhance tolerance against future stresses. This study focused on the metabolomic and transcriptomic changes that occur in proso millet leaves. However, the effects of salt stress on the roots remain unknown. Therefore, further research should seek to understand the influence of re-watering to relieve Na^+ toxicity on roots using these two proso millet cultivars.

Funding

This work was supported by the National Key Research and Development Program of China (nos.2020YFD1000800 and 2020YFD1000803) and the National Natural Science Foundation of China (no. 31371529).

CRediT authorship contribution statement

Yuhao Yuan: Conceptualization, Data curation, Formal analysis, Writing – original draft. **Jiajia Liu:** Methodology, Software. **Qian Ma:** Methodology, Data curation. **Yongbin Gao:** Formal analysis. **Qinghua Yang:** Writing – review & editing, Project administration. **Xiaoli Gao:** Resources, Formal analysis. **Baili Feng:** Project administration, Resources, Formal analysis.

Declaration of competing interest

The authors declare that they have no known competing financial interests or personal relationships that could have appeared to influence the work reported in this paper.

Appendix A. Supplementary data

Supplementary data to this article can be found online at https://doi.org/10.1016/j.jclepro.2021.130205.

References

Albaladejo, I., Meco, V., Plasencia, F., Flores, F.B., Bolarin, M.C., Egea, I., 2017. Unravelling the strategies used by the wild tomato species *Solanum pennellii* to confront salt stress: from leaf anatomical adaptations to molecular responses. Environ. Exp. Bot. 135, 1–12. https://doi.org/10.1016/j.envexpbot.2016.12.003.

Anders, S., Huber, W., 2010. Differential expression analysis for sequence count data. Genome Biol. 11, 10. https://doi.org/10.1186/gb-2010-11-10-r106.

Azeem, A., Wu, Y.Y., Ullah, I., 2017. Photosynthetic response of two okra cultivars under salt stress and re-watering. J. Plant Interact. 12, 67–77. https://doi.org/10.1080/17429145.2017.1279356.

Cappelli, G., Yamac, S.S., Stella, T., Francone, C., Paleari, L., Negri, M., Confalonieri, R., 2015. Are advantages from the partial replacement of corn with second-generation energy crops undermined by climate change? A case study for giant reed in northern Italy. Biomass Bioenergy 80, 85–93. https://doi.org/10.1016/j.biombioe.2015.04.038.

Cuevas, J., Daliakopoulos, I.N., del Moral, F., Hueso, J.J., Tsanis, I.K., 2019. A review of soil-improving cropping systems for soil salinization. Agronomy-Basel. 9, 295. https://doi.org/10.3390/agronomy9060295.

Dawson, I.K., Powell, W., Hendre, P., Bancic, J., Hickey, J.M., Kindt, R., Hoad, S., Hale, I., Jamnadass, R., 2019. The role of genetics in mainstreaming the production of new and orphan crops to diversify food systems and support human nutrition. New Phytol. 224, 37–54. https://doi.org/10.1111/nph.15895.

Erdal, S.C., Eyidogan, F., Ekmekci, Y., 2021. Comparative physiological and proteomic analysis of cultivated and wild safflower response to drought stress and re-watering.

Physiol. Mol. Biol. Plants 27, 281–295. https://doi.org/10.1007/s12298-021-00934-2.
Flowers, T.J., Munns, R., Colmer, T.D., 2015. Sodium chloride toxicity and the cellular basis of salt tolerance in halophytes. Ann. Bot.-London 115, 419–431. https://doi.org/10.1093/aob/mcu217.
Gao, B., Zhang, D.Y., Li, X.S., Yang, H.L., Zhang, Y.M., Wood, A.J., 2015. De novo transcriptome characterization and gene expression profiling of the desiccation tolerant moss *Bryum argenteum* following rehydration, 16, p. 416. https://doi.org/10.1186/s12864-015-1633-y.
Gupta, A., Rico-Medina, A., Cano-Delgado, A.I., 2020. In: The physiology of plant responses to drought, 386, pp. 266–269. https://doi.org/10.1126/science.aaz7614.
Habiyaremye, C., Matanguihan, J.B., Guedes, J.D., Ganjyal, G.M., Whiteman, M.R., Kidwell, K.K., Murphy, K.M., 2017. Proso millet (*Panicum miliaceum* L.) and its potential for cultivation in the Pacific Northwest, U. S.: a review. Front. Plant Sci. 7, 1961. https://doi.org/10.3389/fpls.2016.01961.
Han, L.P., Wang, W.H., Eneji, A.E., Liu, J.T., 2015. Phytoremediating coastal saline soils with oats: accumulation and distribution of sodium, potassium, and chloride ions in plant organs. J. Clean. Prod. 90, 73–81. https://doi.org/10.1016/j.jclepro.2014.11.064.
Hetz, C., 2012. The unfolded protein response: controlling cell fate decisions under ER stress and beyond. Nat. Rev. Mol. Cell Biol. 13, 89–102. https://doi.org/10.1038/nrm3270.
Hoober, J.K., Eggink, L.L., Chen, M., 2007. Chlorophylls, ligands and assembly of light-harvesting complexes in chloroplasts. Photosynth. Res. 97, 387–400. https://doi.org/10.1007/s11120-007-9181-1.
Iglesias, M.J., Terrile, M.C., Windels, D., Lombardo, M.C., Bartoli, C.G., Vazquez, F., Estelle, M., Casalongue, C.A., 2014. MiR393 regulation of auxin signaling and redox-related components during acclimation to salinity in *Arabidopsis*. PLoS One 9, e107678. https://doi.org/10.1371/journal.pone.0107678.
Javed, Q., Wu, Y.Y., Xing, D.K., Ullah, I., Azeem, A., Rasool, G., 2018. Salt-induced effects on growth and photosynthetic traits of *Orychophragmus violaceus* and its restoration through re-watering. Braz. J. Bot. 41, 29–41. https://doi.org/10.1007/s40415-017-0432-x.
Jia, Y.Y., Xiao, W.X., Ye, Y.S., Wang, X.L., Liu, X.L., Wang, G.H., Li, G., Wang, Y.B., 2020. Response of photosynthetic performance to drought duration and re-watering in maize. Agronomy-Basel 10, 533. https://doi.org/10.3390/agronomy10040533.
Kawashima, Y., Watanabe, E., Umeyama, T., Nakajima, D., Hattori, M., Honda, K., Ohara, O., 2019. Optimization of data-independent acquisition mass spectrometry for deep and highly sensitive proteomic analysis. Int. J. Mol. Sci. 20, 5932. https://doi.org/10.3390/ijms20235932.
Kulak, N.A., Geyer, P.E., Mann, M., 2017. Loss-less nano-fractionator for high sensitivity, high coverage proteomics. Mol. Cell. Proteomics 16, 694–705. https://doi.org/10.1074/mcp.O116.065136.
Li, J.F., Zhou, H., Zhang, Y., Li, Z., Yang, Y.Q., Guo, Y., 2020a. The GSK3-like Kinase BIN2 Is a molecular switch between the salt stress response and growth recovery in *Arabidopsis* thaliana. Dev. Cell 55, 367–380. https://doi.org/10.1016/j.devcel.2020.08.005.
Li, W.H., Du, J., Yu, L., 2020b. Function of NHX-type transporters in improving rice tolerance to aluminum stress and soil acidity. Planta 251, 71. https://doi.org/10.1007/s00425-020-03361-x.
Liu, J.X., Howell, S.H., 2016. Managing the protein folding demands in the endoplasmic reticulum of plants. New Phytol. 211, 418–428. https://doi.org/10.1111/nph.13915.
Liu, J.X., Srivastava, R., Che, P., Howell, S.H., 2007. Salt stress responses in *Arabidopsis* utilize a signal transduction pathway related to endoplasmic reticulum stress signaling. Plant J. 51, 897–909. https://doi.org/10.1111/j.1365-313X.2007.03195.x.
Lu, J., Wu, J., Zhang, C., 2021. Cleaner production of salt-tolerance vegetable in coastal saline soils using reclaimed water irrigation: observations from alleviated accumulation of endocrine disrupting chemicals and environmental burden. J. Clean. Prod. 297, 126746. https://doi.org/10.1016/j.jclepro.2021.126746.
Mao, X.Z., Cai, T., Olyarchuk, J.G., Wei, L.P., 2005. Automated genome annotation and pathway identification using the KEGG Orthology (KO) as a controlled vocabulary. Bioinformatics 21, 3787–3793. https://doi.org/10.1093/bioinformatics/bti430.
Meng, J., Xu, T., Wang, Z., Fang, Y., Xi, Z., Zhang, Z., 2014. The ameliorative effects of exogenous melatonin on grape cuttings under water-deficient stress: antioxidant metabolites, leaf anatomy, and chloroplast morphology. J. Pineal Res. 57, 200–212. https://doi.org/10.1111/jpi.12159.
Merlot, A.M., Shafie, N.H., Yu, Y., Richardson, V., Jansson, P.J., Sahni, S., Lane, D.J.R., Kovacevic, Z., Kalinowski, D.S., Richardson, D.R., 2016. Mechanism of the induction of endoplasmic reticulum stress by the anti-cancer agent, di-2-pyridylketone 4,4-dimethyl-3-thiosemicarbazone (Dp44mT): activation of PERK/eIF2a, IRE1a, ATF6 and calmodulin kinase. Biochem. Pharmacol. 109, 27–47. https://doi.org/10.1016/j.bcp.2016.04.001.
Metternicht, G.I., Zinck, J.A., 2003. Remote sensing of soil salinity: potentials and constraints. Remote Sens. Environ. 85, 1–20. https://doi.org/10.1016/S0034-4257(02)00188-8.
Niu, J., Zhang, S.P., Liu, S.D., Ma, H.J., Chen, J., Shen, Q., Ge, C.W., Zhang, X.M., Pang, C.Y., Zhao, X.H., 2018. The compensation effects of physiology and yield in cotton after drought stress. J. Plant Physiol. 224, 30–48. https://doi.org/10.1016/j.jplph.2018.03.001.
Pan, Y., Wang, Z.H., Yang, L., Wang, Z.F., Shi, L., Naran, R., Azadi, P., Xu, F.S., 2012. Differences in cell wall components and allocation of boron to cell walls confer variations in sensitivities of *Brassica napus* cultivars to boron deficiency. Plant Soil 354, 383–394. https://doi.org/10.1007/s11104-011-1074-6.
Qi, F.F., Zha, Z.Y., Du, L., Feng, X.J., Wang, D.N., Zhang, D., Fang, Z.D., Ma, L.J., Jin, Y. D., Xia, C.Q., 2014. Impact of mixed low-molecular-weight organic acids on uranium accumulation and distribution in a variant of mustard (*Brassica juncea var. tumida*). J. Radioanal. Nucl. Chem. 149, 159. https://doi.org/10.1007/s10967-014-3279-7.
Qiao, Y., Jiang, W., Lee, J., Park, B., Choi, M.S., Piao, R., Woo, M.O., Roh, J.H., Han, L.Z., Paek, N.C., Seo, H.S., Koh, H.J., 2010. *SPL28* encodes a clathrin-associated adaptor protein complex 1, medium subunit micro 1 (AP1M1) and is responsible for spotted leaf and early senescence in rice (*Oryza sativa*). New Phytol. 185, 258–274. https://doi.org/10.1111/j.1469-8137.2009.03047.x.
Santos, C.V., 2004. Regulation of chlorophyll biosynthesis and degradation by salt stress in sunflower leaves. Sci. Hortic.-Amsterdam 103, 1. https://doi.org/10.1016/j.scienta.2004.04.009.
Sarwat, M., Naqvi, A.R., 2013. Heterologous expression of rice calnexin (OsCNX) confers drought tolerance in *Nicotiana tabacum*. Mol. Biol. Rep. 40, 5451–5464. https://doi.org/10.1007/s11033-013-2643-y.
Shi, W.M., Yao, J., Yan, F., 2009. Vegetable cultivation under greenhouse conditions leads to rapid accumulation of nutrients, acidification and salinity of soils and groundwater contamination in South-Eastern China. Nutrient Cycl. Agroecosyst. 83, 73–84. https://doi.org/10.1007/s10705-008-9201-3.
Silva, K.J.P., Mahna, N., Mou, Z.L., Folta, K.M., 2018. NPR1 as a transgenic crop protection strategy in horticultural species. Hortic. Res.-England 5, 15. https://doi.org/10.1038/s41438-018-0026-1.
Simura, J., Antoniadi, I., Novak, O., 2018. Plant hormonomics: multiple phytohormone profiling by targeted metabolomics. Plant Physiol. 177, 476–489. https://doi.org/10.1104/pp.18.00293.
Staehelin, L.A., 2003. Chloroplast structure: from chlorophyll granules to supra-molecular architecture of thylakoid membranes. Photosynth. Res. 76, 185–196. https://doi.org/10.1023/A:1024994525586.
Su, L.Y., Dai, Z.W., Li, S.H., Xin, H.P., 2015. A novel system for evaluating drought-cold tolerance of grapevines using chlorophyll fluorescence. BMC Plant Biol. 15, 82. https://doi.org/10.1186/s12870-015-0459-8.
Tan, X.Y., Li, S., Hu, L.Y., Zhang, C.L., 2020. Genome-wide analysis of long non-coding RNAs (lncRNAs) in two contrasting rapeseed (*Brassica napus* L.) genotypes subjected to drought stress and re-watering. BMC Plant Biol. 20, 1. https://doi.org/10.1186/s12870-020-2286-9.
Teo, G.S., Kim, S., Tsou, C.C., Collins, B., Gingras, A.C., Nesvizhskii, A.I., Choi, H., 2015. mapDIA: preprocessing and statistical analysis of quantitative proteomics data from data independent acquisition mass spectrometry. J. Proteonomics 129, 108–120. https://doi.org/10.1016/j.jprot.2015.09.013.
Trapnell, C., Roberts, A., Goff, L., Pertea, G., Kim, D., Kelley, D.R., Pachter, L., 2012. Differential gene and transcript expression analysis of RNA-seq experiments with TopHat and Cufflinks. Nat. Protoc. 7, 562–578. https://doi.org/10.1038/nprot1014-2513a.
Vander, M.K., Turcsan, A., Maes, J., Duchene, N., Meeus, S., Steppe, K., Steenackers, M., 2016. Repeated summer drought and re-watering during the first growing year of oak (*Quercus petraea*) delay autumn senescence and bud burst in the following spring. Front. Plant Sci. 7, 419. https://doi.org/10.3389/fpls.2016.00419.
Wang, M.H., Lee, J.S., Li, Y., 2017. Global proteome profiling of a marine copepod and the mitigating effect of ocean acidification on mercury toxicity after multigenerational exposure. Environ. Sci. Technol. 51, 5820–5831. https://doi.org/10.1021/acs.est.7b01832.
Wang, X.L., Duan, P.L., Yang, S.J., Liu, Y.H., Qi, L., Shi, J., Li, X.L., Song, P., Zhang, L.X., 2020. Corn compensatory growth upon post-drought rewatering based on the effects of rhizosphere soil nitrification on cytokinin. Agric. Water Manag. https://doi.org/10.1016/j.agwat.2020.106436.
Wisniewski, J.R., Zougman, A., Nagaraj, N., Mann, M., 2009. Universal sample preparation method for proteome analysis. Nat. Methods 6, 359–360. https://doi.org/10.1038/NMETH.1322.
Xu, D.H., Su, P.X., Zhang, R.Y., Li, H.L., Zhao, L., Wang, G., 2010. Photosynthetic Parameters and Carbon Reserves of a Resurrection Plant *Reaumuria Soongorica* during Dehydration and Rehydration, vol. 60, pp. 183–190. https://doi.org/10.1007/s10725-009-9440-6. Plant Growth Regul.
Xu, Z.H., Wu, W.R., 2013. Comparative and joint analyses of gene expression profiles under drought and re-watering in *Arabidopsis*. Genet. Mol. Res. 12, 3622–3629. https://doi.org/10.4238/2013.September.13.6.
Yang, Y.Q., Guo, Y., 2018. Unraveling salt stress signaling in plants. J. Integr. Plant Biol. 60, 796–804. https://doi.org/10.1111/jipb.12689.
Young, M.D., Wakefield, M.J., Smyth, G.K., Oshlack, A., 2010. Gene ontology analysis for RNA-seq: accounting for selection bias. Genome Biol. 11, 1–12. https://doi.org/10.1186/gb-2010-11-2-r14.
Yu, H.Y., Ma, Q.H., Liu, X.D., Li, Y.B., Li, L., Qi, M., Wu, W.J., Wang, Y.H., Xu, Z.Z., Zhou, G.S., Zhang, F., 2021. Resistance, recovery, and resilience of desert steppe to precipitation alterations with nitrogen deposition. J. Clean. Prod. 317, 128434. https://doi.org/10.1016/j.jclepro.2021.128434.
Yu, Z.P., Duan, X.B., Luo, L., Dai, S.J., Ding, Z.J., Xia, G.M., 2020. How plant hormones mediate salt stress responses. Trends Plant Sci. 25, 1117–1130. https://doi.org/10.1016/j.tplants.2020.06.008.
Yuan, Y.H., Liu, C.J., Gao, Y.B., Ma, Q., Yang, Q.H., Feng, B.L., 2021. Proso millet (*Panicum miliaceum* L.): a potential crop to meet demand scenario for sustainable saline agriculture. J. Environ. Manag. 296, 113216. https://doi.org/10.1016/j.jenvman.2021.113216.
Zelm, E.V., Zhang, Y.X., Testerink, C., 2020. Salt tolerance mechanisms of plants. Annu. Rev. Plant Biol. 71 https://doi.org/10.1146/annurev-arplant-050718-100005, 24.1-24.31.

Zhang, H., Zhao, Y., Zhu, J.K., 2020. Thriving under stress: how plants balance growth and the stress response. Dev. Cell 55, 529–543. https://doi.org/10.1016/j.devcel.2020.10.012.

Zhang, L., Chen, J.F., Zhou, X., Chen, X.F., Li, Q., Tan, H.X., Dong, X., Xiao, Y., Chen, L. D., Chen, W.S., 2016. Dynamic metabolic and transcriptomic profiling of methyl jasmonate-treated hairy roots reveals synthetic characters and regulators of lignan biosynthesis in *Isatis indigotica* Fort. Plant Biotechnol. J. 14, 2217–2227. https://doi.org/10.1111/pbi.12576.

Zhang, Z.L., Sun, D., Tang, Y., Zhu, R., Li, X., Gruda, N., Dong, J.L., Duan, Z.Q., 2021. Plastic shed soil salinity in China: current status and next steps. J. Clean. Prod. 296, 126453. https://doi.org/10.1016/j.jclepro.2021.126453.

Zhu, J.K., 2016. Abiotic stress signaling and responses in plants. Cell 167, 313–324. https://doi.org/10.1016/j.cell.2016.08.029.

Zou, C.S., Li, L.T., Miki, D., Li, D.L., Tang, Q.M., Xiao, L.H., Rajput, S., Deng, P., Peng, L., Jia, W., Huang, R., Zhang, M.L., Sun, Y.D., Hu, J.M., Fu, X., Schnable, P.S., Chang, Y. X., Li, F., Zhang, H., Feng, B.L., Zhu, X.G., Liu, R.Y., Schnable, J.C., Chnable, J.C., Zhu, J.K., Zhang, H., 2019. The genome of broomcorn millet. Nat. Commun. 10, 436. https://doi.org/10.1038/s41467-019-08409-5.